ACCOUNTS
of chemical research

# Graphene: Powder, Flakes, Ribbons, and Sheets

DUSTIN K. JAMES[†] AND JAMES M. TOUR[*,†,⊥,‡,§]

*Departments of [†]Chemistry, [⊥]Mechanical Engineering and Materials Science, and [‡]Computer Science and the [§]Smalley Institute for Nanoscale Science and Technology, 6100 Main St MS 222, Rice University, Houston, Texas, 77005, United States*

RECEIVED ON APRIL 30, 2012

## CONSPECTUS

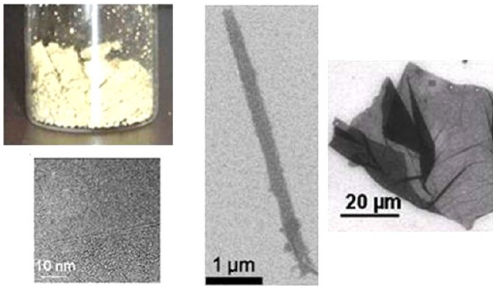


Graphene's unique physical and electrical properties (high tensile strength, Young's modulus, electron mobility, and thermal conductivity) have led to its nickname of "super carbon." Graphene research involves the study of several different physical forms of the material: powders, flakes, ribbons, and sheets and others not yet named or imagined. Within those forms, graphene can include a single layer, two layers, or ≤10 sheets of $sp^2$ carbon atoms. The chemistry and applications available with graphene depend on both the physical form of the graphene and the number of layers in the material. Therefore the available permutations of graphene are numerous, and we will discuss a subset of this work, covering some of our research on the synthesis and use of many of the different physical and layered forms of graphene.

Initially, we worked with commercially available graphite, with which we extended diazonium chemistry developed to functionalize single-walled carbon nanotubes to produce graphitic materials. These structures were soluble in common organic solvents and were better dispersed in composites. We developed an improved synthesis of graphene oxide (GO) and explored how the workup protocol for the synthesis of GO can change the electronic structure and chemical functionality of the GO product. We also developed a method to remove graphene layers one-by-one from flakes. These powders and sheets of GO can serve as fluid loss prevention additives in drilling fluids for the oil industry.

Graphene nanoribbons (GNRs) combine small width with long length, producing valuable electronic and physical properties. We developed two complementary syntheses of GNRs from multiwalled carbon nanotubes: one simple oxidative method that produces GNRs with some defects and one reductive method that produces GNRs that are less defective and more electrically conductive. These GNRs can be used in low-loss, high permittivity composites, as conductive reinforcement coatings on Kevlar fibers and in the fabrication of large area transparent electrodes.

Using solid carbon sources such as polymers, food, insects, and waste, we can grow monolayer and bilayer graphene directly on metal catalysts, and carbon-sources containing nitrogen can produce nitrogen-doped graphene. The resulting graphene can be transferred to other surfaces, such as metal grids, for potential use in transparent touch screens for applications in personal electronics and large area photovoltaic devices. Because the transfer of graphene from one surface to another can lead to defects, low yields, and higher costs, we have developed methods for growing graphene directly on the substrates of interest. We can also produce patterned graphene to make GNRs or graphane/graphene superlattices within a single sheet. These superlattices could have multiple functions for use in sensors and other devices.

This Account only touches upon this burgeoning area of materials chemistry, and the field will continue to expand as researchers imagine new forms and applications of graphene.

## Introduction

Graphene has been called "super carbon"[1] for its intrinsic strength of 130 GPa (extrapolated to graphite), Young's modulus of ~1000 GPa, electron mobility of >200 000 $cm^2/(V\ s)$ and thermal conductivity of >5000 W/(mK).[1] Thousands of graphene papers have been published in China, the United States, and Europe between 2000 and 2012,[1] demonstrating the intense interest in the material. Graphene is in the early stages of commercial production, and scientists and engineers continue to search for new processes that are

Published on the Web 12/31/2012 www.pubs.acs.org/accounts
10.1021/ar300127r 

industrially viable.[2] Research on graphene has advanced to the point that graphene is often being treated "as a reactant rather than a product".[3] Our laboratory has joined in the search for graphene synthesis routes and applications. We have reviewed the synthesis and manipulation of graphene[4] along with the processes to produce graphene oxide and related materials.[5] A tutorial review of the chemical syntheses of graphene nanoribbons developed in our laboratory has also appeared.[6] Here we review our work with graphene powder, flakes, ribbons, and sheets, just a few of its possible forms, and the applications we have found for these materials. In categorizing the papers that are covered in this Account, we approached the body of work as materials chemists and divided the papers by the major form of graphene that was used: powder, flakes, ribbons, or sheets. Each form of graphene has complementary uses.

## Synthesis, Functionalization, and Applications of Graphite and Graphene Oxide

The progression from single-walled carbon nanotube chemistry to graphene chemistry began with an extension of the diazonium functionalization protocols[7] that had been developed for single-walled carbon nanotubes (SWCNTs)[8] by functionalizing chemically converted graphene (CCG), produced from sodium dodecylbenzenesulfonate-wrapped graphene oxide (GO, a material that is produced by oxidation of graphite and exists as exfoliated sheets of carbon that are heavily oxidized[9]) that had been reduced by hydrazine to remove oxygen functional groups and make it more conductive;[10] CCG is therefore graphene that has been synthesized via chemical reaction of a more oxidized or less conjugated carbon material. The functionalized CCGs were readily dispersed in *N*,*N*′-dimethylformamide (DMF), *N*,*N*′-dimethylacetamide, and 1-methyl-2-pyrrolidinone (NMP) in concentrations up to 1 mg/mL. The diazonium chemistry was further utilized to functionalize thermally converted graphene (TCG, produced by rapidly heating GO to 1000 °C to remove most oxygen content[11]) that had been mechanically exfoliated (ground using a mortar and pestle in an ionic liquid to separate the graphene layers).[11] The functionalized TCGs had solubilities in DMF ranging from 0.45 to ∼0.02 mg/mL. The functionalized CCG and functionalized TCG could then potentially be used in producing composites where direct interactions between the additives and the polymeric components are important for producing stronger composite products.

Expanded graphite, which has a solubility of 0.97 mg/mL in chlorosulfonic acid, was functionalized in that solvent using *in situ* diazonium chemistry.[12] Because the sheets of the expanded graphite were exfoliated by the functionalization, it is referred to as chemically assisted exfoliated graphene (CEG). The CEG was mainly edge functionalized with 4-bromophenyl addends, predominantly within 70 nm of the edges, to produce CEG sheets with about 4−10 layers that retain the pristine graphene structure in the interior basal planes. Analysis of the small flakes by transmission electron microscopy indicated that >70% of them had <5 layers and about 10% were monolayer.

The storage of hydrogen in carbon nanomaterials is of great interest for future hydrogen-powered automobiles and the use of functionalized SWCNTs fibers for that purpose has been studied;[13] the 3-D nanoengineered fibers physisorb twice as much hydrogen per unit surface area as do typical macroporous carbon materials. The lower cost of graphene materials and the possibility of achieving higher hydrogen storage capacities encouraged their examination using a similar approach. TCG flakes were annealed at 1000 °C to remove most of the oxygen functionality, and the product was dispersed in chlorosulfonic acid or oleum.[14] *In situ* diazonium functionalization of TCG using a mixture of 4-chloroaniline and 4,4′-methylenedianiline or *tert*-butylaniline alone produced two functionalized materials in which the phenyl rings were also sulfonated by the solvent. The hydrogen uptake of TCG was ∼1.0 wt % per 500 $m^2/g$ at 77 K and 2 bar, while the hydrogen uptake of functionalized-TCG products was ∼1.9 wt % per 500 $m^2/g$ at 77 K and 2 bar, a 2× improvement over prior nanocarbon material hydrogen uptakes.

Graphene is often comprised of several layers; the ability to remove single layers in a predetermined manner is important to the development of graphene materials for applications in electronics. By sputtering of Zn onto the surface of GO, CCG, chemical vapor deposition (CVD) graphene, or mechanically cleaved graphene flakes, followed by dissolution of the Zn with dilute acid, one graphene layer of the flake is removed to leave the lower layers intact (Figure 1).[15] Based on the data produced, the sputtering process damages the top graphene layer and the acid treatment removes the damaged layer. Since the Zn layers can be predesigned patterns, the process can be viewed as single-atomic-layer resolution lithography that can produce graphene-based materials with specific numbers of layers in specific places.

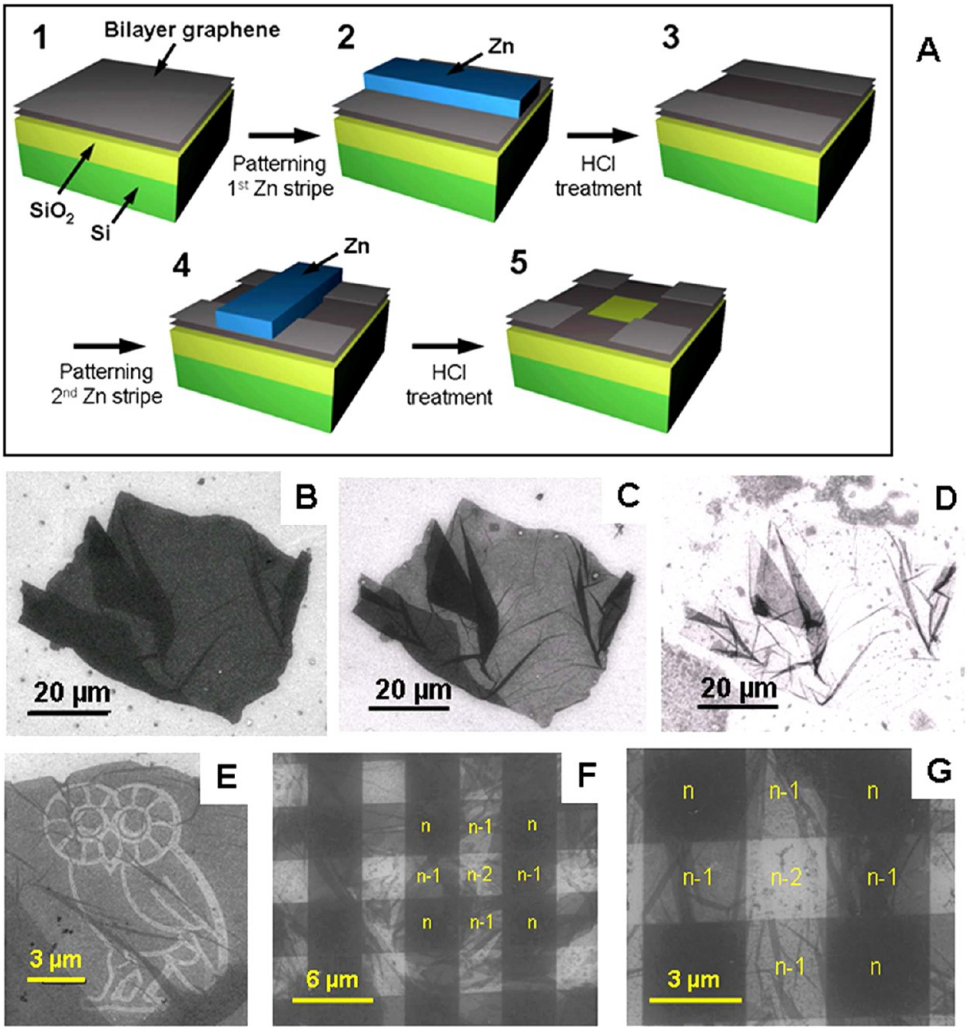


**FIGURE 1.** (A) Schematic illustration of the method for layer-by-layer removal of graphene: (1) the bilayer graphene on top of a $Si/SiO_2$ substrate; (2) a patterned layer of zinc metal is sputtered atop the graphene; (3) the zinc is removed by aqueous HCl (0.02 M) in 3−5 min with simultaneous removal of one graphene layer; (4) patterning of a second zinc stripe; (5) HCl treatment removes the second stripe of zinc plus the underlying carbon layer. (B−D) Scanning electron microscopy (SEM) image of the same bilayer GO flake: (B) original, (C) after the first, and (D) after the second Zn/HCl treatment. (E) SEM image of a monolayer GO flake patterned in the image of an owl. (F, G) SEM images of a continuous GO film patterned with horizontal and vertical stripes in two consecutive Zn/HCl treatments. The lightest squares (an example is marked with "$n-2$"), where the horizontal and vertical stripes overlap, represent areas exposed to two treatments. Areas exposed to one treatment (examples are marked with "$n-1$") are with a shade between the lightest and darkest squares. The darkest squares (examples are marked with "$n$") represent the areas with the original untreated GO film. Caption and Figure from ref 15.

The common method for producing GO, Hummer's method using $KMnO_4$, $NaNO_3$, and $H_2SO_4$, was improved by eliminating the $NaNO_3$, increasing the amount of $KMnO_4$, and using a 9:1 mixture of $H_2SO_4/H_3PO_4$.[16] The improved method did not generate toxic gas, the temperature of the reaction was more easily controlled, and more material was produced that is more heavily oxidized. When the product was reduced to CCG, it had electrical conductivity equivalent to CCG produced by reduction of Hummer's GO.[16]

GO is one of a number of carbon nanomaterials that could be transitioned to commercial products in energy-based applications such as in drilling fluids for downhole oil and gas production. Drilling fluids have a number of functions, including carrying drill cuttings to the surface, supporting the wellbore walls, protecting the underground mixture of hydrocarbons and porous rocks or formations from damage, and creation of a thin low-permeability cake that protects permeable formations.[17] Blockage of hydrocarbon flow paths or formation collapse can be caused by fluid invasion into formations. Fluid-loss-control additives form filter cakes on the wellbore walls to retard the loss of drilling fluid into permeable formations.[17] Graphite, large flake

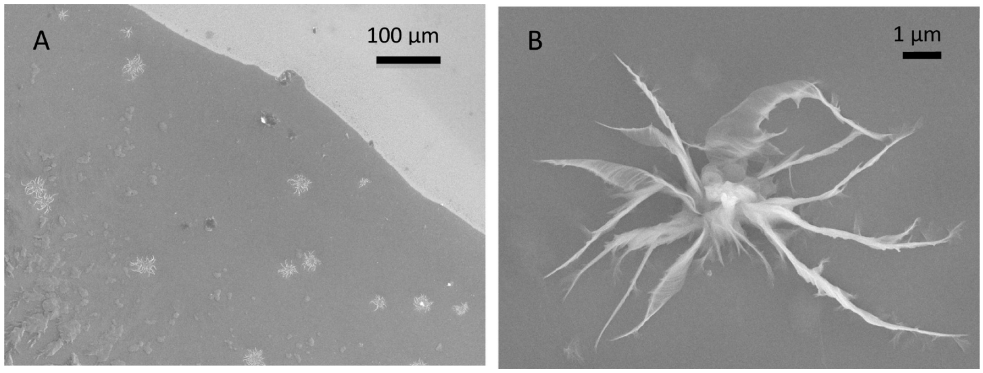


**FIGURE 2.** SEM images of (A) multiple LFGO flakes folded into starfish shapes and (B) a single such particle that entered into a 2.7 $\mu$m diameter pore with 100 psi of applied pressure. Caption and Figure from ref 17. Copyright 2012 American Chemical Society.

graphite (145 $\mu$m), and powdered graphite can be oxidized by $KMnO_4$ to make GO, large flake GO (LFGO), or powdered GO (PGO), respectively. A 3:1 w/w mixture of LFGO/PGO can be used in drilling fluid mixtures to control fluid loss in the formation being drilled.[17] SEM revealed that LFGO flakes by themselves are extremely pliable and are forced by high pressure to crumple and slide through pores with diameters much smaller than the LFGO flake's flattened size (Figure 2). It is thought that the PGO acts as reinforcement of the cake-coating porous formation.[17] As seen in Figure 2B, when individual sheets of LFGO entered pores that are much smaller than the diameter of the flattened LFGO, the flakes crumple and fold into starfish shapes, much like what would occur in a sheet of newspaper forced into a small hole. Molecular modeling confirms and explains the extreme pliability of GO.

While the synthesis of GO is well-known, the detailed chemical structure of the material is not; there are several structural models that interpret the experimental data. The models are different and do not agree as to the type and number of functional groups present in conventional GO.[18] A well-controlled study using organic solvents instead of water to workup the reaction has now established that it is not the type of graphite used or the oxidation protocol that determines the final GO structure and properties but rather the quenching and purification procedures (Figure 3).[18] Pristine GO is the material that is first produced under the standard oxidation conditions. The introduction of water into the workup procedure causes stepwise conversion of tertiary alcohols into ketones, where the electrons lost by the ionized hydrogen atoms are used to extend the conjugated areas. The ketones that terminate the large vacancy defects are in equilibrium with their hydrated forms. The changes in structure introduced by the workup with water result in the final conventional GO product. The acidic properties of conventional GO samples can be partially explained by the presence of incompletely hydrolyzed covalent sulfates; the presence of carboxylic acid groups cannot be ruled out by the data in this study.[18]

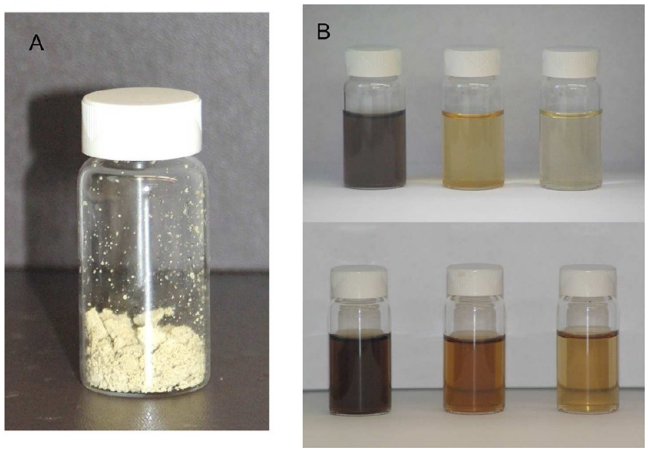


**FIGURE 3.** Photographs of the light-colored GO samples. (A) A photograph of dry GO worked up in trifluoroacetic acid. (B) A photograph of the as-prepared aqueous solutions (top) of the following GO samples (left to right): conventional GO, GO worked up in methanol, and GO worked up in trifluoroacetic acid. On the bottom: the same solutions after 24 h. The concentration of the solutions was 0.5 mg/mL. Note how dark the conventional GO solution is, while the solutions of the GO worked up in nonaqueous conditions are much lighter but still darken on aging and exposure to light. Darkening occurs as the flakes become more conjugated. Figure partially reproduced from ref 18. Copyright 2012 American Chemical Society.

## Oxidation of MWCNTs to Graphene Nanoribbons

Thin, elongated strips of graphene that possess straight edges, graphene nanoribbons (GNRs), change from semiconductors to semimetals as their width is increased; hence they represent a particularly versatile variety of graphene.

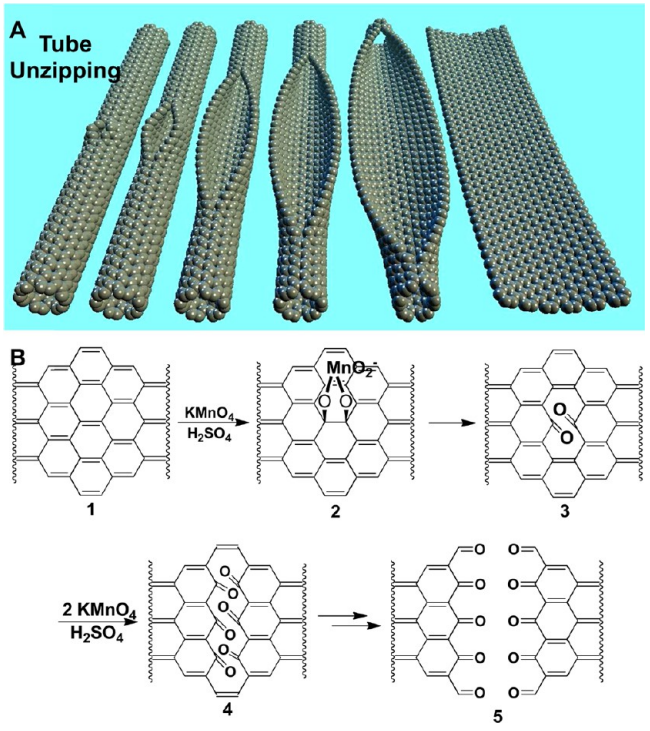


**FIGURE 4.** (A) Schematic representation of the gradual unzipping of one wall of a carbon nanotube by the action of $KMnO_4$ in $H_2SO_4$ to form a nanoribbon; oxygen atoms are not shown. (B) The proposed chemical mechanism of nanotube unzipping. Figure reproduced in part from ref 19.

A solution-based oxidative process that produces a nearly 100% yield of GNRs (weight of carbon in and out) has been developed that involves the treatment of multiwalled carbon nanotubes (MWCNTs) suspended in concentrated $H_2SO_4$ with 5 wt equiv of $KMnO_4$[19] to produce graphene oxide nanoribbons (GONRs, Figure 4) that are then chemically reduced to GNRs. The GONRs are water-soluble. To prevent reaggregation of the GNRs after the reduction, the GONRs were suspended in sodium dodecyl sulfate (SDS). The conductivities of the GNRs (~300 nm wide) were similar to that obtained from other wide exfoliated or CVD GNRs.[20] Mounting evidence suggests that unzipping is akin to splitting by intercalation of chemical species between MWCNT layers. The SWCNTs, having no differing layers, seem to be more resistant to this splitting. Subsequently an improved optimized method for producing GONRs from MWCNTs was developed.[21] The GONRs have fewer defects or holes in the basal plane, exemplified by their higher conductivity compared with those originally made;[19] GONRs < 100 nm were produced, and the high aspect ratio was maintained. The key to the improved procedure was the introduction of a second, weaker acid into the system that apparently improves the selectivity of the oxidation by *in situ* protection of the vicinal diols formed on the basal place of the graphene during the oxidation, thereby preventing their over oxidation and subsequent hole generation.[21]

Diazonium functionalization chemistry was again used to solubilize a carbon nanomaterial, in this case the GNRs produced through chemical reduction of GONRs in SDS.[22] The reduction and functionalization reactions were done in one flask to simplify the process. The successful functionalization indicated that the GONRs were partially rearomatized in the reduction to GNRs since the diazonium species are expected to react only at $sp^2$ carbons. The solubility of the functionalized GNRs in DMF and NMP ranged from ~0.2 to ~0.1 mg/mL. The GNR functionalizaton chemistry was put to further use in fabricating thin films that were assembled on SiOx/Si surfaces to fabricate bottom-gated GNR thin-film transistors via a solution process that produced 20−80 bilayers of negatively or positively charged GNR films.[23] The bilayers were produced by a simple dip, rinse, dry, and dip process, depositing the thin films on a pretreated glass surface. The GNR thin film field-effect transistors demonstrated only p-type behavior. The conductivity was better than GO-based devices but not as good as similar devices made from mechanically cleaved, CVD, or epitaxially grown graphene.[23] The kinetics of the diazonium functionalization of GNRs, produced by chemical reduction of GONRs followed by annealing at 900 °C, was measured by probing the electrical properties of the GNRs fabricated into devices.[24] The diazonium functionialization was done after the annealing. The high temperature of the anneal was needed to remove the oxygen functionality that had been introduced in the GONR synthesis. It was found that functionalization with 4-nitrobenzene diazonium tetrafluoroborate was quite fast, with >60% of the maximum change in electrical properties observed in <5 min of grafting at room temperature.

Monolayer nonfunctionalized GNRs fabricated into electronic devices[25] demonstrated lower conductivity (~35 S/cm) and mobility of charge carriers (0.5−3 $cm^2/(V\ s)$) than the conductivity and mobility of pristine graphene, even though the GNRs (made by oxidation of MWCNTs using $KMnO_4$) had been chemically reduced and then annealed in $Ar/H_2$ at 900 °C. The $KMnO_4$ oxidation produces too many defects and holes that are not healed by reduction and annealing. Electron spin resonance investigation of GNRs that had been produced by chemically reducing GONRs with hydrazine or hydrogen indicated the presence of C-based free radical centers that exhibited paramagnetic features,[26] thus providing further support for the findings that chemical reduction

processes do not remove all of the defects and holes from GONRs. However, careful annealing of GONRs using three consecutive timed high-temperature treatments does produce larger intrinsic energy bandgaps in the resulting GNRs.[27,28] Direct measurements were made of intrinsic energy bandgaps of ~50 meV in GNRs ~100 nm wide. High-resolution TEM and Raman spectroscopy, in combination with an absence of hopping conductance and stochastic charging effects, suggested low defect density.[27]

Pristine MWCNTs offer poor reinforcement in epoxy-based composites due to shielding of the polymer matrix from contact with the internal tubes by the outermost tubes, poor wetting and interfacial adhesion, and intertube slip via a sword-in-sheath type failure of the concentric nanotube cylinders.[29] The use of GNRs made via annealing of GONRs at 1050 °C in epoxy composites[29] produced a ~30% increase in Young's modulus at ~0.3 wt % fraction compared with MWCNTs. The ultimate tensile strength, also at ~0.3 wt % fraction, showed a ~22% improvement compared with MWCNTs. Thus GNRs can be used as high-performance additives in composites with properties similar to those of SWCNTs composites but at lower cost.

## MWCNTs Split by Potassium Vapor To Form Ribbons

It has been shown that the synthesis of GNRs through the oxidation of MWCNTs by $KMnO_4$ followed by one annealing step produces material that is relatively high in defects and is not as conductive as graphene from mechanically cleaved graphite. Thus, a route to more highly conductive GNRs was sought, and it was found that splitting pristine MWCNTs using potassium vapor produced GNRs that were free of oxidized surfaces and could be prepared in large batches in 100% yield (Figure 5).[30] The GNRs produced from potassium splitting (K-GNRs) could be exfoliated in a subsequent treatment in chlorosulfonic acid. The ~7000 to ~9000 S/cm electrical conductivity of these low-defect K-GNRs was comparable to that of graphene from mechanically cleaved graphite. Sodium vapor did not produce any splitting. The origins of the directionally selective splitting of the MWCNTs were explored using computer modeling to present an explanation for the unique role of potassium in this reaction.[30] The lower defect K-GNRs were used in the fabrication of large area transparent electrodes[31] by dispersing the K-GNRs in either chlorosulfonic acid or aqueous SDS at a concentration of 1 mg/mL. The dispersions were spray-coated onto glass slides; spin-coating or blade coating did not work as well. The slides with the chlorosulfonic acid dispersed K-GNRs were immersed in hot ethanol (80 °C) followed by a 1:1 vol/vol mixture of ethanol/water (80 °C, 5 min) to remove the acid, while the films produced from the aqueous SDS dispersions were immersed in 50% $H_2SO_4$ for 5 s followed by soaking in 1:1 vol/vol ethanol/water at 80 °C for 1 h to remove the SDS; the washing procedure was critical since the unwashed films from the aqueous SDS dispersions were almost nonconductive.[31] The films produced from the K-GNRs/chlorosulfonic acid dispersion were 10× more conductive than those produced from the K-GNRs/aqueous SDS dispersion at the same transmittance. SEM analysis indicated that the K-GNRs were more highly aggregated in the SDS dispersions and that the K-GNRs were more exfoliated in the films from the chlorosulfonic acid dispersion. There was thus lower K-GNR contact resistance in the films from chlorosulfonic acid; the resistance was as low as 800 Ω/□ when the transmittance at 550 nm was 78%.[31]

The K-GNRs were used to make low-loss, high-permittivity composites[32] for use in radio and microwave antennas and other military applications, where low signal loss from the composites covering the electronics is important. The K-GNRs were suspended in chloroform, and the suspension was mixed with a chloroform solution of NuSil part A two-part elastomer. After horn-sonication of the K-GNR/NuSil A mixture and removal of the solvent (simple mechanical blending of the K-GNRs into the NuSil part A did not produce adequate dispersion), part B of the NuSil was added, and the two parts were manually stirred; after placing the mixture in a mold and degassing under vacuum to remove trapped air, the elastomer was cured in a 100 °C oven for 2 h. By varying the content of the conductive filler, the loss and permittivity could be tuned to desirable values over a wide range, producing composites useful for different applications. In another application, SWCNTs, MWCNTs or K-GNRs were coated onto Kevlar fibers[33] by spray coating *ortho*-dichlorobenzene dispersions of the nanomaterials onto polyurethane-coated Kevlar fibers at 200 °C. The polyurethane served as a binder for the nanomaterials; other polymer-based binders such as epoxy did not work as well. The SWCNT-coated Kevlar fiber had the highest conductivity of 65 S/cm while the MWCNT-coated fiber's conductivity was 9 S/cm and the K-GNR-coated fiber had a conductivity of 20 S/cm. The SWCNT-coated fiber had a knot efficiency (calculated by dividing the breaking strength of a knotted fiber by the breaking strength of the fiber without knotting) of 23%, more than four times higher than that of carbon

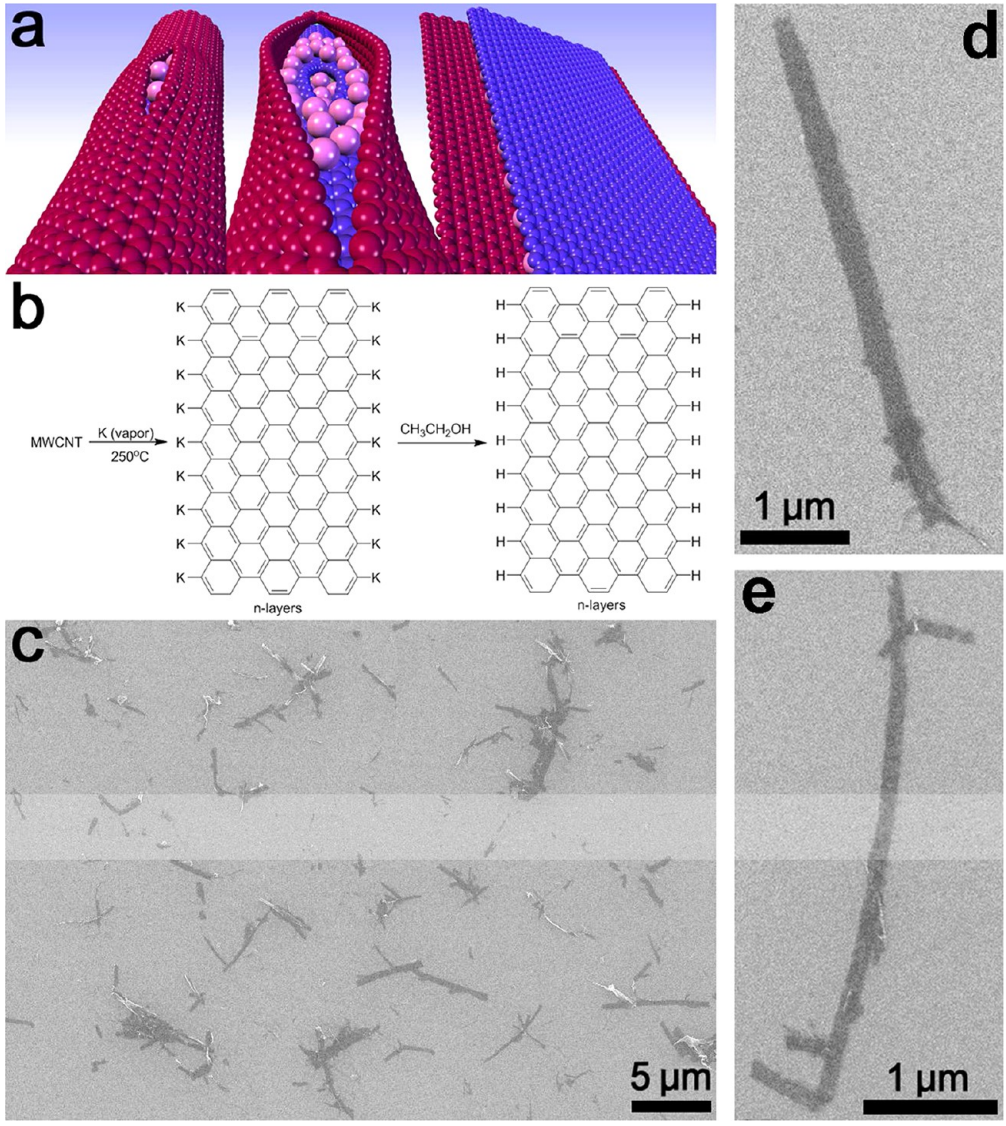


**FIGURE 5.** (a) A schematic of potassium intercalation between the nanotube walls and sequential longitudinal splitting of the walls followed by unraveling to a nanoribbon stack. The potassium atoms along the periphery of the ribbons are excluded for clarity. (b) A chemical schematic of the splitting processes where ethanol is used to quench the aryl potassium edges; only a single layer is shown for clarity while the actual number of K-GNR layers correlates with the number of concentric tubes in the MWCNT. (c) An overview of a large area showing complete conversion of MWCNTs to K-GNRs. (d, e), Images of isolated K-GNR stacks demonstrating characteristic high aspect ratios and predominantly parallel edges. Caption and Figure reproduced from ref 30. Copyright 2011 American Chemical Society.

fibers, and it could be bent or dipped into water multiple times without loss of conductivity.

## Growth of Graphene Sheets from Solid Carbon Sources

Graphene is a quite stable form of carbon as is shown by the growth of graphene on a Cu catalyst film from simple carbon sources such as poly(methyl methacrylate) (PMMA), fluorene, and sucrose (Figure 6).[34] The PMMA was deposited on the Cu as a film while fine powders of fluorene or sucrose were used; monolayer graphene was obtained by heating to at least 800 °C, with a maximum temperature studied of 1000 °C. A reductive flow of $H_2$/Ar gas at low pressure was used both to reduce the starting materials and to sweep away extruded C atoms and other byproducts. Under the same conditions, few-layer graphene was also grown on a Ni film while neither graphene nor amorphous carbon was obtained on Si or $SiO_2$ substrates. This demonstrates the potential to grow patterned graphene from a thin film of shaped metal catalyst deposited directly on $SiO_2$/Si wafers without postlithographic treatment, because PMMA-derived graphene will not grow on the Si of $SiO_2$ surfaces.[34]

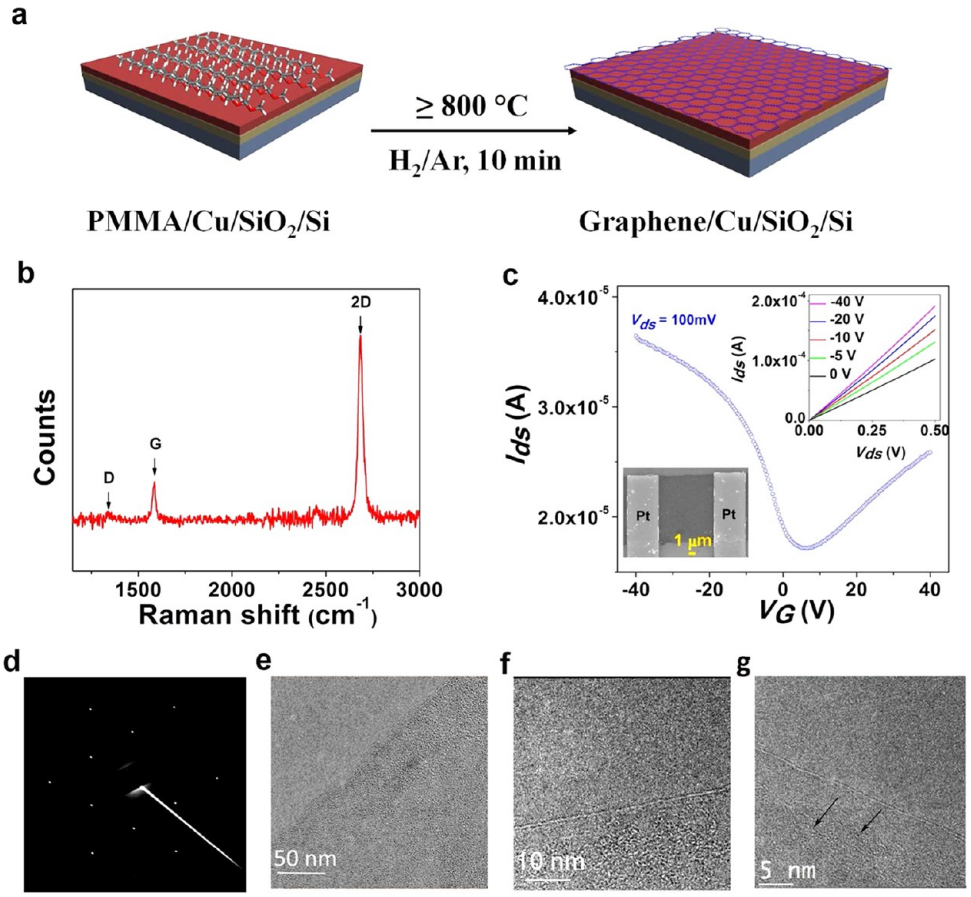


**FIGURE 6.** (a) Monolayered graphene is derived from the solid PMMA films on Cu substrates at 800 °C or higher, up to 1000 °C. (b) Raman spectrum (514 nm excitation) of a monolayered graphene obtained at 1000 °C. (c) Room temperature $I_{ds}-V_G$ curve on a graphene-based back-gate FET device. The upper inset shows the $I_{ds}-V_{ds}$ characteristics as a function of $V_G$. $V_G$ changes from 0 V (bottom) to −40 V (top). The lower inset in panel c is the SEM (JEOL-6500 microscope) image of this device where the graphene is perpendicular to the Pt leads. (d) SAED pattern of graphene. (e, f, g) HRTEM images of graphene films. Black arrows in panel g indicate the Cu atoms. Caption and Figure from ref 34.

A nitrogen doping agent, melamine ($C_3N_6H_6$), could be mixed with the PMMA and the mixture spin coated onto the Cu surface to produce N-doped graphene under the same temperature and gas flow conditions (except at atmospheric pressure). The doped graphene had an N content of 2 to 3.5%. Nitrogen-doped graphene could also be grown by using pyridine as the source of both the carbon and the nitrogen in a CVD process.[35] In all cases, the graphene had to be transferred from the catalyst surface to another surface such as $SiO_2$ or Si in order to use it to make devices. For instance, graphene produced from PMMA can be transferred onto $SiO_2$ on which a prior self-assembled monolayer (SAM) had been deposited;[36] the SAMs produce controlled doping of the graphene with little effect on its mobility, and the assembly is more stable than conventional noncovalent dopants. Additionally, PMMA-derived graphene can be transferred to a $SiO_2$ device and the surface then coated with poly(ethylene imine)/poly(ethylene glycol) films, which produce a controlled ambipolar-to-unipolor conversion.[37]

The PMMA-derived graphene can be transferred atop a metal grid on glass or poly(ethylene terephthalate) to produce transparent films[38] with sheet resistance as low as 3 Ω/□ and transmittance at ∼80%. At 90% transmittance, the sheet resistance was ∼20 Ω/□. Both values are among the best for transparent electrode materials to date. Because the materials used are earth-abundant stable elements, their potential usefulness for replacement of indium tin oxide (ITO) in many applications is increased due to the cost of ITO.[38]

Indeed, it has been found that graphene can be produced from common carbon-containing materials such as food, plastic, insects, and waste (Figure 7).[39] The carbon source materials, without prepurification, were placed on a Cu foil that was then heated to 1050 °C under a $H_2$/Ar flow. The graphene grew on the backside of the Cu foil and the

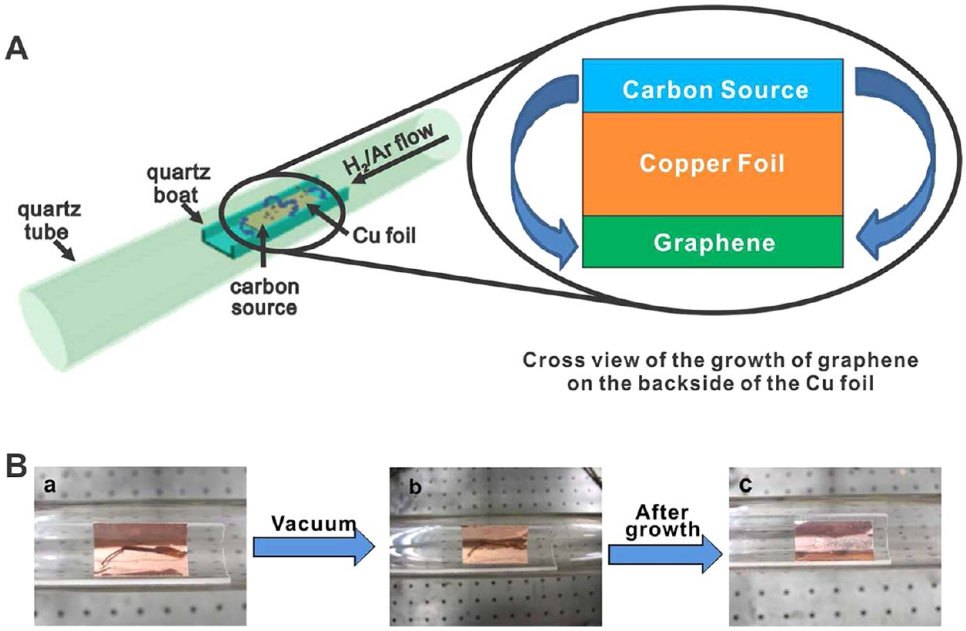


**FIGURE 7.** (A) Diagram of the experimental apparatus for the growth of graphene from food, insects, or waste in a tube furnace. On the left, the Cu foil with the carbon source contained in a quartz boat is placed at the hot zone of a tube furnace. The growth is performed at 1050 °C under low pressure with a $H_2$/Ar gas flow. On the right is a cross view that represents the formation of pristine graphene on the backside of the Cu substrate. (B) Growth of graphene from a cockroach leg. (a) One roach leg on top of the Cu foil. (b) The roach leg under vacuum. (c) The residue from the roach leg after annealing at 1050 °C for 15 min. The pristine graphene grew on the bottom side of the Cu film (not shown). Caption and Figure reproduced from ref 39. Copyright 2011 American Chemical Society.

nonvolatile pyrolyzed species remaining on the frontside of the Cu foil were removed when the foil was etched away. The backside of the foil with the graphene layer was coated with PMMA before the Cu was etched away in order to transfer the graphene to another surface. The monolayer graphene that was produced was of high quality as determined by Raman spectroscopy, X-ray photoelectron spectroscopy (XPS), ultraviolet—visible spectroscopy, and TEM analyses.[39]

The reader will note that transfer of the graphene sheet from the surface on which it is grown to another surface is necessary for the aforementioned applications. A process that produces graphene that does not need to be transferred to another surface would be useful in order to minimize damage and reduce cost since each transfer takes time, reduces yield, and increases the potential for error. Further research has produced processes that do not require graphene transfer. PMMA and high-impact polystyrene (gas-phase $CH_4$ can also be used as a carbon source) can be deposited atop a 400-nm-thick layer of Ni on a $SiO_2$ substrate; heating to 1000 °C produces decomposition and diffusion of the carbon sources through the Ni.[40] Upon cooling to room temperature, bilayer graphene was formed between the $SiO_2$ substrate and the Ni, which can be subsequently removed by an etchant to leave the graphene deposited on the $SiO_2$. Raman spectroscopy mapping indicated that the graphene was high quality and bilayer coverage was ~70%. In a similar process, carbon sources such as films of poly(2-phenylpropyl)methysiloxane, poly(methyl methacrylate), polystyrene, and poly(acrylonitrile-*co*-butadiene-*co*-styrene) (the latter leading to N-doped bilayer graphene due to its inherent nitrogen content) or from a self-assembled monolayer of butyltriethoxysilane (atop a $SiO_2$ layer) were deposited on insulating surfaces such as $SiO_2$, h-BN, $Si_3N_4$, and $Al_2O_3$.[41] Heating the assembly to 1000 °C under low pressure and a reducing atmosphere produced bilayer graphene between the Ni layer and the insulating substrate. The Ni layer was removed by dissolution, affording the bilayer graphene directly on the insulator. Since no transfer step was needed, loss and contamination of the graphene was reduced.

## Patterned Graphene Sheets

The controllable and reversible modification of properties in graphene by patterning or chemical functionalization can modulate the graphene's optical and electronic properties. CVD graphene could be converted into GNRs directly on device substrates by patterning the graphene with CuO

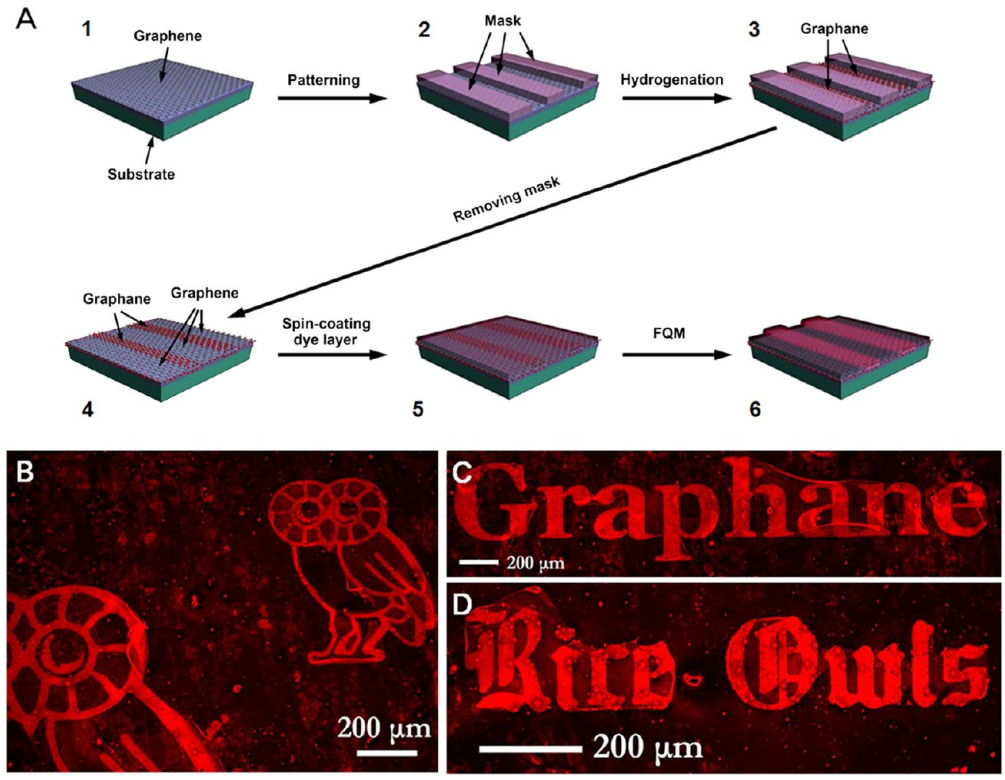


**FIGURE 8.** (A) Schematic illustration of the fabrication of the graphane/graphene superlattices and subsequent FQM imaging. Standard photolithography with a photoresist or e-beam lithography with a PMMA mask was used to produce the images. (B–D) Different graphane/graphene patterns were made on the graphene that were imaged by FQM. Figure from ref 43.

nanowires.[42] The CuO nanowires were spin-coated onto the graphene from a liquid dispersion. Reactive ion etching was used to remove the graphene not protected by the nanowires, and the nanowires were then dissolved in dilute HCl. Depending on the duration of the plasma etching, the fabricated GNR devices exhibited either standard ambipolar electric field effects or p-type transistor behaviors with ON–OFF ratios >50.

The ability to controllably pattern graphane/graphene superlattices within a single sheet of graphene has been experimentally demonstrated (Figure 8) by reducing graphene to graphane via hydrogenation of masked areas.[43] By exchanging the $sp^3$ C–H bonds in graphane with $sp^3$ C–C bonds through functionalization, sophisticated multifunctional superlattices can be fabricated on both the macroscopic and microscopic scales. These patterns were visualized using fluorescence quenching microscopy (FQM)[44] techniques and confirmed using Raman spectroscopy. By tuning the extent of hydrogenation, the density of the $sp^3$ C functional groups on graphene's basal plane can be controlled from 0.4% to 3.5%.[43] With such a technique, which allows for both spacial and density control of the functional groups, a route to multifunctional specifically patterned recognition sites might be realized across a single graphene sheet, facilitating the development of graphene-based devices.

## Conclusion

The synthesis, functionalization, and application of carbon nanomaterials such as graphite, graphene, GO, GNRs, and other products has rapidly advanced. Additionally, methods have been found to produce graphene from simple and inexpensive materials and to reduce the number of steps needed to manipulate the carbon nanomaterals in order to use them in applications. Graphene research across the globe is quickly moving forward as researchers develop new strategies in this exciting area of chemical research.[45]

*The Advanced Energy Consortium (BG Group, Halliburton, Conoco Phillips, bp, OXY, Marathon, Shell, Total, Petrobras, Schlumberger), the Lockheed Martin Corporation through the LANCER IV Program, Air Force Office of Scientific Research (Grant FA9550-09-1-0581), Air Force Research Laboratory through University Technology Corporation (Grant 09-S568-064-01-C1), the US Department of Energy's Office of Energy Efficiency and Renewable Energy within the Hydrogen Sorption Center of Excellence (Grant DE-FC-36-05GO15073), the Office of Naval Research through a MURI with*

*the University of California, Berkeley (Grant 00006766, N00014-09-1-1066), the Army Research Office (Grant No. W911NF-08-C-0133) through a SBIR to PrivaTran LLC, M-I SWACO (a Schlumberger Company), Sandia National Laboratory, and the American Chemical Society through the Arthur C. Cope Award provided funding for this work.*

**Supporting Information.** Table of acronym definitions. This material is available free of charge via the Internet at http://pubs.acs.org.

## BIOGRAPHICAL INFORMATION

**Dustin K. James** graduated with a B.S. in Chemistry from Southwestern University, Georgetown, Texas, and with a Ph.D. in Organic Chemistry from The University of Texas at Austin, where his advisor was James K. Whitesell. After 16 years in the pharmaceutical, specialty chemical, and semiconductor wastewater treatment industries, he came to Rice in 2001, where he is a Research Scientist/Laboratory Manager.

**James M. Tour**, a synthetic organic chemist, is presently the T. T. and W. F. Chao Professor of Chemistry, Professor of Computer Science, and Professor of Mechanical Engineering and Materials Science. Tour's scientific research areas include a diversity of nanomaterials and nanomedicine topics. He was ranked one of the Top 10 chemists in the world over the past decade by a Thomson Reuters citations per publication index survey and recently received the first *ACS Nano* Lectureship award for the Americas. Tour has over 475 research publications and over 60 patents. http://www.jmtour.com.

## FOOTNOTES

*E-mail tour@rice.edu, fax 713-348-6250.
The authors declare no competing financial interest.

## REFERENCES

1 Savage, N. Super Carbon. *Nature* **2012**, *483*, S30–S31.
2 Van Noorden, R. Beyond Sticky Tape. *Nature* **2012**, *483*, S32–S33.
3 Ruoff, R. A Means to an End. *Nature* **2012**, *483*, S42.
4 Sun, Z.; James, D. K.; Tour, J. M. Graphene Chemistry: Synthesis and Manipulation. *J. Phys. Chem. Lett.* **2011**, *2*, 2425–2432.
5 Sinitskii, A.; Tour, J. M. Chemical Approaches to Produce Graphene Oxide and Related Materials. In *Graphene Nanoelectronics: From Materials to Circuits*; Murali, R., Ed.; Springer: New York, 2012; DOI 10.1007/978-1-4614-0548-1_8.
6 James, D. K.; Tour, J. M. The Chemical Synthesis of Graphene Nanobribbons—A Tutorial Review. *Macromol. Chem. Phys.* **2012**, *213*, 1033–1050.
7 Bekyarova, E.; Itkis, M. E.; Ramesh, P.; Berger, C.; Sprinkle, M.; de Heer, W. A.; Haddon, R. C. Chemical Modification of Epitaxial Graphene: Spontaneous Grafting of Aryl Groups. *J. Am. Chem. Soc.* **2009**, *131*, 1336–1337.
8 Dyke, C. A.; Tour, J. M. Feature Article: Covalent Functionalization of Single-Walled Carbon Nanotubes for Materials Applications. *J. Phys. Chem. A* **2004**, *108*, 11151–11159.
9 Hummers, W. S.; Offeman, R. E. Preparation of Graphitic Oxide. *J. Am. Chem. Soc.* **1958**, *80*, 1339.
10 Lomeda, J. R.; Doyle, C. D.; Kosynkin, D. V.; Hwang, W.-H.; Tour, J. M. Diazonium Functionalization of Surfactant-Wrapped Chemically Converted Graphene Sheets. *J. Am. Chem. Soc.* **2008**, *130*, 16201–16206.
11 Jin, Z.; Lomeda, J. R.; Price, B. P.; Lu, W.; Zhu, Y.; Tour, J. M. Mechanically Assisted Exfoliation and Functionalization of Thermally Converted Graphene Sheets. *Chem. Mater.* **2009**, *21*, 3045–3047.
12 Sun, Z.; Kohama, S.; Zhang, Z.; Lomeda, J. R.; Tour, J. M. Soluble Graphene through Edge-Selective Functionalization. *Nano Res.* **2010**, *3*, 117–125.
13 Leonard, A. D.; Hudson, J. L.; Fan, H.; Booker, R.; Simpson, L. J.; O'Neill, K. J.; Parilla, P. A.; Heben, M. J.; Pasquali, M.; Kittrell, C.; Tour, J. M. Nanoengineered Carbon Scaffolds for Hydrogen Storage. *J. Am. Chem. Soc.* **2009**, *131*, 723–738.
14 Jin, Z.; Lu, W.; O'Neill, K. J.; Parilla, P. A.; Simpson, L. J.; Kittrell, C.; Tour, J. M. Nano-Engineered Spacing in Graphene Sheets for Hydrogen Storage. *Chem. Mater.* **2011**, *23*, 923–925.
15 Dimiev, A.; Kosynkin, D. V.; Sinitskii, A.; Slesarev, A.; Sun, Z.; Tour, J. M. Layer-by-Layer Removal of Graphene for Device Patterning. *Science* **2011**, *331*, 1168–1172.
16 Marcano, D. C.; Kosynkin, D. V.; Berlin, J. M.; Sinitskii, A.; Sun, Z.; Slesarev, A.; Alemany, L. B.; Lu, W.; Tour, J. M. Improved Synthesis of Graphene Oxide. *ACS Nano* **2010**, *4*, 4806–4814.
17 Kosynkin, D. V.; Ceriotti, G.; Wilson, K. C.; Lomeda, J. R.; Scorsone, J. T.; Patel, A. D.; Friedheim, J. E.; Tour, J. M. Graphene Oxide as a High-Performance Fluid-Loss-Control Additive in Water-Based Drilling Fluids. *ACS Appl. Mater. Interfaces* **2012**, *4*, 222–227.
18 Dimiev, A.; Kosynkin, D. V.; Alemany, L. B.; Chaguine, P.; Tour, J, M. Pristine Graphite Oxide. *J. Am. Chem. Soc.* **2012**, *134*, 2815–2822.
19 Kosynkin, D. V.; Higginbotham, A. L.; Sinitskii, A.; Lomeda, J. R.; Dimiev, A.; Price, B. K.; Tour, J. M. Longitudinal Unzipping of Carbon Nanotubes to Form Graphene Nanoribbons. *Nature* **2009**, *458*, 872–826.
20 Li, X.; Wang, X.; Zhang, L.; Lee, S.; Dai, H. Chemically Derived, Ultrasmooth Graphene Nanoribbon Semiconductors. *Science* **2008**, *319*, 1229–1232.
21 Higginbotham, A. L.; Kosynkin, D. V.; Sinitskii, A.; Sun, Z.; Tour, J. M. Low-Defect Graphene Oxide Nanoribbons from Multiwalled Carbon Nanotubes. *ACS Nano* **2010**, *4*, 2059–2069.
22 Zhu, Y.; Higginbotham, A. L.; Tour, J. M. Covalent Functionalization of Surfactant-Wrapped Graphene Nanoribbons. *Chem. Mater.* **2009**, *21*, 5284–5291.
23 Zhu, Y.; Tour, J. M. Graphene Nanoribbon Thin Films Using Layer-by-Layer Assembly. *Nano Lett.* **2010**, *10*, 4356–4362.
24 Sinitskii, A.; Dimiev, A.; Corley, D. A.; Fursina, A. A.; Kosynkin, D. V.; Tour, J. M. Kinetics of Diazonium Functionalization of Chemically Converted Graphene Nanoribbons. *ACS Nano* **2010**, *4*, 1949–1954.
25 Sinitskii, A.; Fursina, A. A.; Kosynkin, D. V.; Higginbotham, A. L.; Natelson, D.; Tour, J. M. Electronic Transport in Monolayer Graphene Nanoribbons Produced by Chemical Unzipping of Carbon Nanotubes. *Appl. Phys. Lett.* **2009**, *95*, No. 253108.
26 Rao, S. S.; Stesmans, A.; Kosynkin, D. V.; Higginbotham, A.; Tour, J. M. Paramagnetic Centers in Graphene Nanoribbons Prepared from Longitudinal Unzipping of Carbon Nanotubes. *New J. Phys.* **2011**, *13*, No. 113004.
27 Shimizu, T.; Haruyama, J.; Marcano, D. C.; Kosynkin, D. V.; Tour, J. M.; Hirose, K.; Suenaga, K. Large Intrinsic Energy Bandgaps in Annealed Nanotube-Derived Graphene Nanoribbons. *Nat. Nanotechnol.* **2011**, *6*, 45–50.
28 Han, M. L.; Özyilmaz, B.; Zhang, Y.; Kim, P. Energy Band-Gap Engineering of Graphene Nanoribbons. *Phys. Rev. Lett.* **2007**, *98*, No. 206805.
29 Rafiee, M. A.; Lu, W.; Thomas, A. V.; Zandiatashbar, A.; Rafiee, J.; Tour, J. M.; Koratkar, N. A. Graphene Nanoribbon Composites. *ACS Nano* **2010**, *4*, 7415–7420.
30 Kosynkin, D. V.; Lu, W.; Sinitskii, A.; Pera, G.; Sun, Z.; Tour, J. M. Highly Conductive Graphene Nanoribbons by Longitudinal Splitting of Carbon Nanotubes Using Potassium Vapor. *ACS Nano* **2011**, *5*, 968–974.
31 Zhu, Y.; Lu, W.; Sun, Z.; Kosynkin, D. V.; Yao, J.; Tour, J. M. High Throughput Preparation of Large Area Transparent Electrodes Using Non-Functionalized Graphene Nanoribbons. *Chem. Mater.* **2011**, *23*, 935–939.
32 Dimiev, A.; Lu, W.; Zeller, K.; Crowgey, B.; Kempel, L. C.; Tour, J. M. Low-Loss, High-Permittivity Composites Made from Graphene Nanoribbons. *ACS Appl. Mater. Interfaces* **2011**, *3*, 4657–4661.
33 Xiang, C.; Lu, W.; Zhu, Y.; Sun, Z.; Yan, Z.; Hwang, C.-C.; Tour, J. M. Carbon Nanotube and Graphene Nanoribbon-Coated Conductive Kevlar Fibers. *ACS Appl. Mater. Interfaces* **2012**, *4*, 131–136.
34 Sun, Z.; Yan, Z.; Yao, J.; Beitler, E.; Zhu, Y.; Tour, J. M. Growth of Graphene from Solid Carbon Sources. *Nature* **2010**, *468*, 549–552.
35 Jin, Z.; Yao, J.; Kittrell, C.; Tour, J. M. Large-Scale Growth and Characterizations of Nitrogen-Doped Monolayer Graphene Sheets. *ACS Nano* **2011**, *5*, 4112–4117.
36 Yan, Z.; Sun, Z.; Lu, W.; Yao, J.; Zhu, Y.; Tour, J. M. Controlled Modulation of Electronic Properties of Graphene by Self-Assembled Monolayers on $SiO_2$ Substrates. *ACS Nano* **2011**, *5*, 1535–1540.
37 Yan, Z.; Yao, J.; Sun, Z.; Zhu, Y.; Tour, J. M. Controlled Ambipolar-to-Unipolar Conversion in Graphene Field-Effect Transistors Through Surface Coating with Poly(ethylene imine)/Poly(ethylene glycol) Films. *Small* **2012**, *8*, 59–62.
38 Zhu, Y.; Sun, Z.; Yan, Z.; Jin, Z.; Tour, J. M. Rational Design of Hybrid Graphene Films for High-Performance Transparent Electrodes. *ACS Nano* **2011**, *8*, 6472–6479.
39 Ruan, G.; Sun, Z.; Peng, Z.; Tour, J. M. Growth of Graphene from Food, Insects, and Waste. *ACS Nano* **2011**, *5*, 7601–7607.

40 Peng, Z.; Yan, Z.; Sun, Z.; Tour, J. M. Direct Growth of Bilayer Graphene on $SiO_2$ Substrates by Carbon Diffusion through Nickel. *ACS Nano* **2011**, *5*, 8241–8247.

41 Yan, Z.; Peng, Z.; Sun, S.; Yao, J.; Zhu, Y.; Liu, Z.; Ajayan, P. M.; Tour, J. M. Growth of Bilayer Graphene on Insulating Substrates. *ACS Nano* **2011**, *5*, 8187–8192.

42 Sinitskii, A.; Tour, J. M. Patterning Graphene Nanoribbons Using Copper Oxide Nanowires. *Appl. Phys. Lett.* **2012**, *100*, No. 103106.

43 Sun, Z.; Pint, C. L.; Marcano, D. C.; Zhang, C.; Yao, J.; Ruan, G.; Yan, Z.; Zhu, Yu.; Hauge, R. H.; Tour, J. M. Towards Hybrid Superlattices in Graphene. *Nat. Commun.* **2011**, *2*, No. 559.

44 Kim, J.; Cote, L. J.; Kim, F.; Huang, J. Visualizing Graphene Based Sheets by Fluorescence Quenching Microscopy. *J. Am. Chem. Soc.* **2010**, *132*, 260–267.

45 Liang, Y. T.; Hersam, M. C. Towards Rationally Designed Graphene-Based Materials and Devices. *Macromol. Chem. Phys.* **2012**, *213*, 1091–1100.